MITSUBISHI ELECTRIC RESEARCH LABORATORIES
http://www.merl.com

Macrocell-Wide Behavior of the Orthogonality Factor in WCDMA Downlinks

Neelesh Mehta, Andreas Molisch, Larry Greenstein

TR2006-102 December 2006

Abstract

The orthogonality factor (OF) quantifies the loss of orthogonality between the signals transmitted simultaneously on a wideband code division multiple access (WCDMA) downlink due to multipath dispersion. It is one of the fundamental parameters that determines the signal-to-interference-plus-noise ratio at the output of the Rake receiver and, consequently, it has a significant impact on downlink system capacity. The OF depends greatly on the delay profile of the multipath channel between the mobile and its serving base station; this profile varies considerably from one location in the cell to another. In this paper, we study how the statistical properties of the small-scale-fading-averaged OF vary over the entire macrocellular area. We use an ensemble of channel profiles at different locations in a cell generated from an implementation of the comprehensive COST259 channel model, which incorporates results from several experimental investigations. We show that the small-scale-fading-averaged OF is itself a random variable whose statistics depend on the mobile's distance from its serving base station. The large observed variance of the OF indicates that using a single value for all users in downlink capacity analyses and simulations, as has been the practice, may lead to erroneous conclusions. Finally, we propose a simple model that closely matches the statistics of the OF as a function of mobile-to-base distance, thus obviating the need to set up the complicated channel model every time OF values are to be generated.

IEEE Transactions on Wireless Communications (2006)

Macrocell-Wide Behavior of the Orthogonality Factor in WCDMA Downlinks

Neelesh B. Mehta, *Senior Member, IEEE*, Andreas F. Molisch, *Fellow, IEEE*, and Larry J. Greenstein, *Life Fellow, IEEE*

***Abstract*— The *orthogonality factor (OF)* quantifies the loss of orthogonality between the signals transmitted simultaneously on a wideband code division multiple access (WCDMA) downlink due to multipath dispersion. It is one of the fundamental parameters that determines the signal-to-interference-plus-noise ratio at the output of a Rake receiver and, consequently, it has a significant impact on downlink system capacity. The OF depends greatly on the delay profile of the multipath channel between the mobile and its serving base station; this profile varies considerably from one location in the cell to another.**

In this paper, we study how the statistical properties of the small-scale-fading-averaged OF vary over the entire macrocellular area. We use an ensemble of channel profiles at different locations in a cell generated from an implementation of the comprehensive COST259 channel model, which incorporates results from several experimental investigations. We show that the small-scale-fading-averaged OF is itself a random variable whose statistics depend on the mobile's distance from its serving base station. The large observed variance of the OF indicates that using a single value for all users in downlink capacity analyses and simulations, as has been the practice, may lead to erroneous conclusions. Finally, we propose a simple model that closely matches the statistics of the OF as a function of mobile-to-base distance, thus obviating the need to set up the complicated channel model every time OF values are to be generated.

***Index Terms*— Cellular radio, channel profile, COST259, fading channels, land mobile radio propagation factors, multipath channels, orthogonality factor, Rake receivers, radio receivers, Rayleigh channels, statistics, time-varying channels, wideband code division multiple access.**

I. INTRODUCTION

THE orthogonality factor (OF) is an important parameter affecting the capacity of third generation cellular systems based on wideband code division multiple access (WCDMA). In downlink capacity analyses and simulations [1]–[4], it measures the intra-cell interference from the loss in orthogonality of the spreading codes due to multipath dispersion. The spreading codes used in WCDMA are a concatenation of pseudo-random long scrambling sequences and short orthogonal channelization sequences.

Manuscript received March 3, 2005; revised January 25, 2006; accepted March 28, 2006. The associate editor coordinating the review of this letter and approving it for publication was M. Sawahashi. A part of this work was presented at Globecom 2005, St. Louis, MO, Nov. 28–Dec.2, 2005.

N. B. Mehta and A. F. Molisch are with Mitsubishi Electric Research Labs (MERL), 201 Broadway, Cambridge, MA 02139 USA. A. F. Molisch is also at the Dept. of Electroscience, Lund Univ., Sweden. L. J. Greenstein is with WINLAB, Rutgers University, 671 Route 1 South, Piscataway, NJ 08902 USA. A part of this work was done when the authors were with AT&T Labs – Research, Middletown, NJ USA (e-mail: mehta@merl.com; molisch@merl.com; ljg@winlab.rutgers.edu).

Digital Object Identifier 10.1109/TWC.2006.05146

The lower the value of the OF, the lower the intra-cell interference, e.g., an OF of 0 corresponds to no interference and an OF of 1 corresponds to considerable downlink interference. Values between 0.1 and 0.6 are common in downlink performance analyses and simulations [2], [3], [5], [6]. The OF influences many important characteristics of a WCDMA system, such as its downlink pole capacity [3], the maximum number of voice users that it can support, and the data throughput experienced by users of the downlink shared channel. Some studies have shown that it can even halve the average throughput experienced by data users [1]. An increase in the OF also adversely affects the downlink pole capacity, with the exact impact depending on the channel load of neighboring cells, use of macro- and antenna diversity, etc. Therefore, a complete characterization of the OF is essential in cell capacity analysis and planning.

The value of the OF depends on the channel delay profile, chip pulse shape, the number of Rake fingers in the receiver, etc. A general and exact analytical expression for the OF was derived in [7] as a function of the channel's instantaneous multipath fade gains and relative delays. Given that the formula is directly a function of the instantaneous fade gains and delays, its accuracy does not depend on the delay profile, fading distributions, and Doppler spectrum, which together determine the time-variation of the instantaneous fade gains. The accuracy of the formula was verified in [7] by looking at several channel profiles defined in the third generation partnership project (3GPP) [8]. The results showed that the channel's delay profile determines the statistical properties of the OF to the greatest extent, and parameters such as the chip pulse shape and number of Rake fingers play a lesser role. This inter-relationship between the orthogonality factor and the delay profile – captured by means of a single parameter called the diversity factor – was further illuminated in [9], [10], which established a simple affine relationship between the two.

Channel measurement analyses, such as those by Greenstein *et al.* [11], show that the dispersion encountered in a given environment statistically increases with the distance of the mobile from the base station (BS). Furthermore, it is correlated with shadowing [11], [12]. Measurement results have also shown that in some environments, multipath components are not always uniformly spread out. Instead, due to the presence of far scatterers, they arrive in clusters [13]–[15], whose relative delays depend on the position of the mobile. Therefore, the delay profile, and consequently the OF, can be quite different for locations spaced far apart.

This paper quantifies the behavior of the OF over an entire cell area. For this purpose, we use the COST259 stochastic-geometric macrocellular channel model proposed by the European Cooperation on Science and Technology (COST) project. The model is among the most comprehensive models available currently [16]–[18]. It builds upon the COST231 studies, is widely supported for realistic simulations of WCDMA, and incorporates the results of several extensive measurement campaigns, e.g., [11], [12], [15], [19]. While using stored traces or ray-tracing methods leads to very accurate channel descriptions, as they can incorporate most of the details of the radio environment, their results are location-specific and can suffer from a lack of generality. What COST259 fundamentally provides is a systematic method to stochastically generate the experimentally observed delay profiles encountered over an entire cell. To account for the different terrains in which cells can be located, COST259 specifies four generic environments, as discussed later. It models the observed interrelation between the large-scale and small-scale behavior of the channel, and includes the above-mentioned Greenstein model. Another notable feature is its explicit modeling of multiple clusters. The COST259 model has also been adopted in the standards [8, Annex A], and has contributed significantly to the 3GPP spatial channel model [20].

The distance dependence of the OF was also observed in [21], which used the Greenstein model. However, it did not take multiple clusters into account and did not characterize the distribution of the OF over a cell area. Another difference is that it used the OF formula of [22], which is different from ours and assumes a different Rake finger weighting scheme. Ray-tracing simulations over an urban area were used in [22], [23], which observed a high correlation between the logarithm of the OF and the logarithm of the multipath delay decay time constant. However, the variation with distance was not modeled. The studies in [24], [25] used actual channel measurements and observed a wide variability in the time-averaged OF. However, the definition of the OF in [24] seems to be based on the ratio of the fading-averaged signal power to the fading-averaged interference plus noise power, which is different from the one in this paper.

We show that the time-averaged OF is itself a random variable that strongly depends on the mobile's distance from the BS. The results we obtain provide a comprehensive characterization of the OF over the entire cell area in all the typically encountered macrocellular environments. We also present an empirical formula to match the observed statistics. The results show that, contrary to the current widespread use of a single orthogonality factor for all users in system capacity analyses, the OF exhibits, for all environments, a surprisingly wide range of values over a cell.

The paper is organized as follows: Section II briefly describes the COST259 channel model (for macrocells) and the analytical results on the OF that we use in this paper. The statistics of the OF for channel profiles generated from COST259 are presented and analyzed in Section III. Section IV summarizes our findings.

II. Background

A. COST259 Channel Model for Macrocells

COST259 is a parametric stochastic model that characterizes the small-scale and the large-scale behavior of the wireless channel, and attempts to integrate previous published and unpublished work on channel modeling and measurements into a single general framework. It simultaneously models many of the important parameters of the channel and their inter-relationships. The parameters modeled are the path loss, shadow fading, short-term fading, temporal and angular dispersion, and polarization. Also incorporated in the model is the empirical observation that the multipath components are not uniformly spread over time and directions of arrival and departure, but are instead clustered.

For a given mobile location, the delay profile in COST259 is determined as follows: The scatterer clusters, corresponding to structures such as buildings and mountains, are distributed over the cell area. Each scatterer cluster has associated with it multiple "visibility regions" in the cell. Each visibility region is a circle of radius R_C. The probability distributions that determine the placing of the scatterers and their corresponding visibility regions are specified in [16], [18]. A mobile located within a scatterer's visibility region experiences multipath dispersion due to that scatterer cluster. This results in a multipath cluster in the mobile's delay profile. The parameters of the cluster are determined as described in the next paragraph. The location of the mobile thus determines the number of non-line-of-sight clusters in its channel impulse response. In addition, there always exists one cluster due to local scattering near the mobile. As the mobile moves, it may enter new visibility regions and leave old ones; thus, its multipath channel profile also dynamically changes, albeit at larger distances.

In addition, the multipath components undergo independent, time-correlated fading that depends on the Doppler frequencies. Each cluster consists of uniformly spaced multipath components. The power of each multipath within a cluster decays exponentially as a function of its relative delay from the first multipath of the cluster. The power of each cluster also decays exponentially as a function of its excess path delay, which is the delay of the first path of the cluster relative to the first path of the first cluster. Once the excess path delay exceeds a 10 μsec threshold, there is no further decay in the cluster power. The power profile as a function of the directional coordinates of the multipath components has also been specified, but is beyond the scope of this paper.

A similar mechanism allows for the occurrence of at most one line-of-sight (LOS) component and determines its power. The probability that an LOS component exists decreases linearly with the distance of the MS from the BS; it vanishes beyond a cut-off distance of 500 m and increases as the height of the BS increases. The shadowing is specified to be the same for all the components of a cluster, and follows a log-normal distribution. However, it is independent between clusters.

The exponential delay profile, $P_n(\tau)$, of the n^{th} cluster, with initial time offset τ_n, is characterized by the delay decay constant, $\sigma_{n\tau}$, as follows:

$$P_n(\tau) = \frac{1}{\sigma_{n\tau}} \exp\left(-\frac{\tau - \tau_n^c}{\sigma_{n\tau}}\right), \quad \text{for } \tau \geq \tau_n^c. \qquad (1)$$

The delay decay constant of the n^{th} cluster, in turn, depends on the distance, r, of the mobile from the BS as follows:

$$\sigma_{n\tau} = m_{s\tau} \left(\frac{r}{1000}\right)^{\epsilon} 10^{0.1 s_{s\tau} Z_m}, \tag{2}$$

where $m_{s\tau}$ is the median value at a distance $r = 1000$ m, $s_{s\tau}$ is the standard deviation expressed in dB, and ϵ is the distance exponent. Z_m is a zero-mean, unit-variance Gaussian random variable that is correlated with a similar Gaussian random variable used for generating the lognormal shadowing. Therefore, the delay decay constant of a cluster is itself a random variable and is correlated with the cluster's shadow fading. The root mean square (rms) delay spread of the entire resultant channel profile thus depends on the number of constituent multipath clusters, their individual delay decay constants, and their relative time delays.

COST259 specifies four generic environments to characterize the macrocellular environment, namely, Generalized Typical Urban (GTU), Generalized Bad Urban (GBU), Generalized Rural Area (GRA), and Generalized Hilly Terrain (GHT). GTU describes cities and towns with buildings having mostly homogeneous height and density, while GBU is a more dispersive environment and describes cities with distinctly inhomogeneous building heights or densities. GRA describes farmlands, fields, and forests with few buildings. GHT is like GRA except with large height variations due to hills or mountains.

B. Orthogonality Factor

Let N denote the number of resolvable multipath components in the channel profile; let α_i denote the complex baseband multipath fading gain of path i $(1 \le i \le N)$; let $\psi(t)$ denote the chip pulse shape and T_c the chip duration. Then the instantaneous OF, conditioned on the multipath fades $\{\alpha_i\}_{i=1}^{N}$, is given by [7]

$$\beta_o(\alpha_1,\ldots,\alpha_N) = \frac{\left[\begin{array}{l} \sum_{\Omega_1} \alpha_{n_1}^* \alpha_{l_1} \alpha_{n_2} \alpha_{l_2}^* \hat{R}_{\psi\psi}(\tau'_{l_1 n_1}) \hat{R}_{\psi\psi}^*(\tau'_{l_2 n_2}) \\ \quad + \sum_{\Omega_1} \alpha_{n_1}^* \alpha_{l_1} \alpha_{n_2} \alpha_{l_2}^* R_{\psi\psi}(\tau'_{l_1 n_1}) R_{\psi\psi}^*(\tau'_{l_2 n_2})] \\ \quad + \sum_{\Omega_2} \alpha_{n_1}^* \alpha_{l_1} \alpha_{n_2} \alpha_{l_2}^* [\hat{R}_{\psi\psi}(\tau'_{l_2 n_2}) R_{\psi\psi}^*(\tau'_{l_2 n_2})] \\ \quad + \sum_{\Omega_3} \alpha_{n_1}^* \alpha_{l_1} \alpha_{n_2} \alpha_{l_2}^* [R_{\psi\psi}(\tau'_{l_2 n_2}) \hat{R}_{\psi\psi}^*(\tau'_{l_2 n_2})] \end{array}\right]}{\left|\sum_{n=1}^{N} \alpha_n \alpha_n^*\right|^2}, \tag{3}$$

where * denotes complex conjugate. In the above equation, Ω_1, Ω_2, and Ω_3 specify the ordered quadruples that arise in the expression for intra-cell interference, and are given by

$$\Omega_1 = \{(l_1,n_1,l_2,n_2) : \theta_{l_1 n_1} = \theta_{l_2 n_2}, l_1 \neq n_1, l_2 \neq n_2, \\ 1 \le l_1, l_2 \le N, 1 \le n_1, n_2 \le N\}, \tag{4}$$

$$\Omega_2 = \{(l_1,n_1,l_2,n_2) : \theta_{l_1 n_1} = \theta_{l_2 n_2} + 1, l_1 \neq n_1, l_2 \neq n_2, \\ 1 \le l_1, l_2 \le N, 1 \le n_1, n_2 \le N\}, \tag{5}$$

$$\Omega_3 = \{(l_1,n_1,l_2,n_2) : \theta_{l_1 n_1} = \theta_{l_2 n_2} - 1, l_1 \neq n_1, l_2 \neq n_2, \\ 1 \le l_1, l_2 \le N, 1 \le n_1, n_2 \le N\}. \tag{6}$$

$\theta_{l_i n_j}$ and $\tau'_{l_i n_j}$ are the integral and fractional chip delays, respectively, and are defined as $\theta_{l_i n_j} = \left\lfloor \frac{\tau_{l_i} - \tau_{n_j}}{T_c} \right\rfloor$ and $\tau'_{l_i n_j} = \tau_{l_i} - \tau_{n_j} - \theta_{l_i n_j} T_c$. $R_{\psi\psi}(\tau')$ and $\hat{R}_{\psi\psi}(\tau')$ are partial pulse correlation functions, and are given by

$$R_{\psi\psi}(\tau') = \int_{-\infty}^{\infty} \psi(t)\psi(t-\tau')dt, \tag{7}$$

$$\hat{R}_{\psi\psi}(\tau') = \int_{-\infty}^{\infty} \psi(t)\psi(t+T_c-\tau')dt. \tag{8}$$

An intuitive feel for the above general formula can obtained by looking at the case in which the multipath delays are integer multiples of the chip duration and a full Rake receiver (which assigns a finger to each resolvable multipath) is used. For this case, the formula simplifies to

$$\beta_o(\alpha_1,\ldots,\alpha_N) = 1 - \frac{\sum_{i=1}^{N} |\alpha_i|^4}{\left(\sum_{i=1}^{N} |\alpha_i|^2\right)^2}, \tag{9}$$

where $|.|$ denotes the absolute value.

In this paper, which considers a large number of delay profiles, we study the properties of the time-averaged or small-scale-fading-averaged OF, $\overline{\beta_o}$, over an entire cell area. The average is evaluated numerically by Monte Carlo averaging of the instantaneous OF (given by (3)) over the small-scale fading, which includes Rayleigh and Ricean fading, but not shadowing or path loss variations.[1] This average value is of interest as most WCDMA system simulations typically use the time-averaged OF [1], [2].

III. OF and COST259 Implementation and Results

A. Implementation Details

The recommended set of parameters in [16] were utilized in the implementation of the COST259 model used here. While COST259 specifies several parameters, the main ones that directly affect the multipath delay profile, such as the average number of multipath clusters, median cluster delay spread, delay spread distance exponent, etc., are listed in Table I for all the four environments. The radii of the macrocells were chosen as 10 km for GRA and GHT (suburban terrain), and 1 km for GBU and GTU (metropolitan terrain). The OF was calculated for a rectangular pulse shape and a full Rake receiver (all paths processed). Note that the chip pulse shape and the number of fingers in the receiver have only a marginal impact on the OF [7], making the results in this paper approximately applicable to partial Rake receivers and systems with other chip pulse shapes, as well.

For a given scatterer and visibility region configuration, the mobile location was determined as follows: For a given distance, r, from the BS, the mobile was placed at 500 randomly generated locations in the cell. The distances of the mobile from the BS were chosen to be $0.1d, 0.2d, \ldots, 1.0d$, where d is the cell radius. Given that COST259 prescribes a stochastic recipe for placing the scatterers and their visibility regions, three different realizations of the placements (using the distribution prescribed by COST259) were considered. A

[1] We shall use time-averaged and small-scale-fading-averaged interchangeably henceforth.

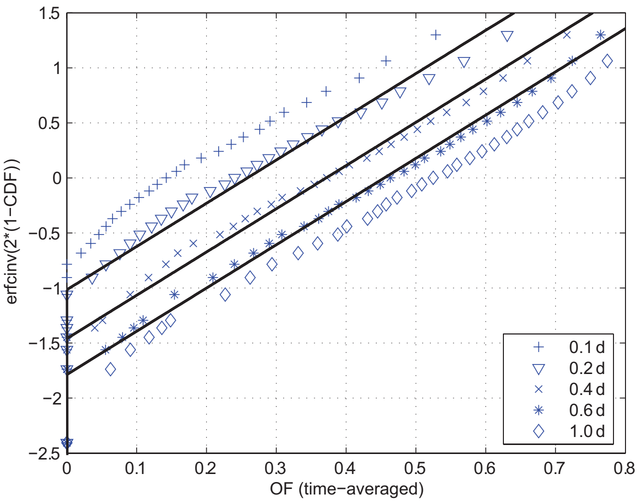

Fig. 1. Generalized Rural Area environment: CDF plotted on 'Gaussian probability scale' as a function of distance from BS. The straight lines (–) are linear curve-fits for $r = 0.2d$, $0.4d$, and $0.6d$.

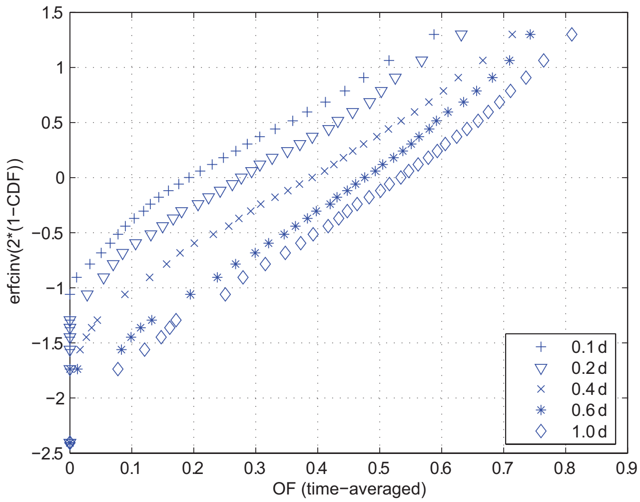

Fig. 2. Generalized Hilly Terrain environment: CDF plotted on 'Gaussian probability scale' as a function of distance from BS.

different set of channel profiles (and consequently a different OF) was obtained in each realization.

For each of the channel profiles generated, $\overline{\beta}_o$ was computed using the method of Sec. II-B. In view of the dependence of the cluster delay decay constant on r, the statistics of $\overline{\beta}_o$ were tabulated as different functions of r.

B. Distance-Dependent Model for $\overline{\beta}_o$

Figure 1 plots the cumulative distribution function (CDF), $F(\overline{\beta}_o)$, of $\overline{\beta}_o$ for the GRA environment. Specifically, we show $\mathrm{erfcinv}(2(1 - F(\overline{\beta}_o)))$ vs. $\overline{\beta}_o$, where erfcinv is the inverse complementary error function and $F(\overline{\beta}_o)$ is the probability that the time-averaged OF is below $\overline{\beta}_o$. The vertical axis is called a Gaussian probability scale because, for a Gaussian random variable, X, with mean μ and standard deviation σ, we have the following linear relationship: $\mathrm{erfcinv}(2(1 - F(x))) = \frac{x-\mu}{\sqrt{2}\sigma}$. The plots are given at each of several distances of the mobile from the BS. In the same manner, Figures 2, 3, and 4 plot the CDFs of $\overline{\beta}_o$ for the GHT, GTU, and GBU environments, respectively.

For all four environments, the qualitative behavior is the same. As the distance, r, increases, the CDF of $\overline{\beta}_o$ shifts to the right. This is because the median value of the delay decay constant of the clusters increases with r. This increases the dispersiveness of the channel, begetting an increase in $\overline{\beta}_o$. It is also of interest to note that, even for a given r, a wide range of values of $\overline{\beta}_o$ is encountered over the cell area, in all four environments. For example, for the GTU environment, for $r = 0.2d$, the 25-percentile value of $\overline{\beta}_o$ is 0.174, while the 75-percentile value is 0.459, which is considerably higher. When $r = 0.6d$, they increase to 0.395 and 0.653, respectively, which again is a wide spread.

It can be seen that the GBU environment exhibits higher values for the OF than the GTU environment. This is due to the presence of twice as many clusters, on average, for GBU than for GTU. Similarly, the GHT environment, which is more dispersive than the GRA environment, has higher OF

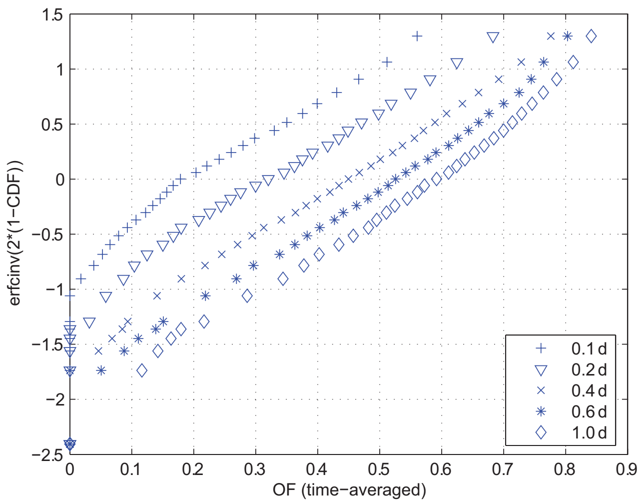

Fig. 3. Generalized Typical Urban environment: CDF plotted on 'Gaussian probability scale' as a function of distance from BS.

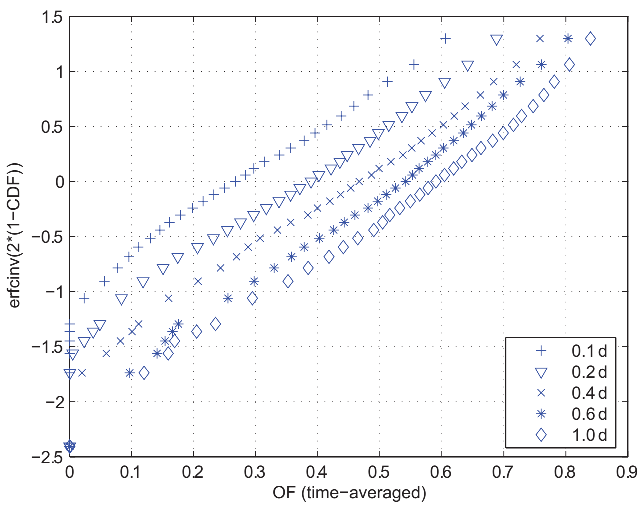

Fig. 4. Generalized Bad Urban environment: CDF plotted on 'Gaussian probability scale' as a function of distance from BS.

TABLE I
IMPORTANT PARAMETERS IN THE COST259 MODEL FOR MACROCELLS

Parameter	GTU	GRA	GHT	GBU
Carrier freq. [GHz]	2.0	2.0	2.0	2.0
BS height [m]	30.0	50.0	50.0	50.0
Mobile height [m]	1.5	1.5	1.5	1.5
Ave. rooftop height [m]	15.0	-	-	30.0
Building separation	30 m	-	-	50 m
Width of roads	15 m	-	-	25 m
Ave. no. of clusters	1.17	1.06	2.00	2.18
Shadow fading dB standard deviation	6.0	6.0	6.0	6.0
Median cluster delay decay constant	0.4	0.1	0.1	0.4
Standard deviation in dB of cluster delay decay constant ($s_{s\tau}$)	3.0	3.0	3.0	3.0
Delay decay constant distance exponent	0.5	0.5	0.5	0.5
Shadowing and delay decay constant correlation	0.5	0.5	0.5	0.5
Visibility region radius [m]	100.0	100.0	100.0	100.0
Multipath component spacing [μsec]	0.26	0.26	0.26	0.26

values. Among the four environments, GBU has, on average, the highest OF values while GRA has the lowest.

Observe that, for each of the four environments, the plots are nearly (but not perfectly) linear. This is especially true for larger distances (where the OFs are larger and thus matter more). We infer from this that, for a given r, a Gaussian distribution may be used to approximate the probability distribution of $\overline{\beta}_o$. If the straight line $y = p_1(r)x + p_2(r)$ is used as the curve-fitting approximation, with y being the ordinate and x the abscissa, then the Gaussian mean and standard deviation of $\overline{\beta}_o$ are given by $\mu(r) = -\frac{p_2(r)}{p_1(r)}$ and $\sigma(r) = \frac{1}{\sqrt{2}p_1(r)}$. Another observation is that the plots are essentially shifted versions of each other (i.e., have essentially the same slopes), which suggests that a distance-independent standard deviation can be used to model the distribution of $\overline{\beta}_o$, with only a marginal loss in curve-fitting accuracy.

This is illustrated in Fig. 1, in which the curve-fitted lines are shown along with the observed values for $r = 0.2d$, $0.4d$, and $0.6d$. The lines are drawn so as to minimize the rms curve-fitting errors (but all lines have the same slope). As the Gaussian distribution must be truncated because $0 \leq \overline{\beta}_o \leq 1$, very small values of the OF (less than 0.01) were not used in the curve-fit; including them would incorrectly skew the slope and the y-intercept of the line. The rms curve-fitting erros, for all distances and environments, range from 0.05 to 0.12. While lines do not provide a perfect fit, they do suggest that a linear fit is a good approximation. Therefore, for the purpose of coming up with a simple, yet descriptive, model of the OF as a function of the mobile-to-base distance, the linear curve-fit is a reasonably accurate model.

Therefore, $\overline{\beta}_o$ for an MS at a distance of r from the BS can be approximated by

$$\overline{\beta}_o = \begin{cases} \mu(r) + \sigma\eta, & -\frac{\mu(r)}{\sigma} \leq \eta \leq \frac{1-\mu(r)}{\sigma} \\ 0, & \text{otherwise} \end{cases}, \quad (10)$$

where η is a zero-mean, unit-variance, Gaussian random variable, $\sigma = 0.180$, and $\mu(r)$ is a monotonically increasing function of r.

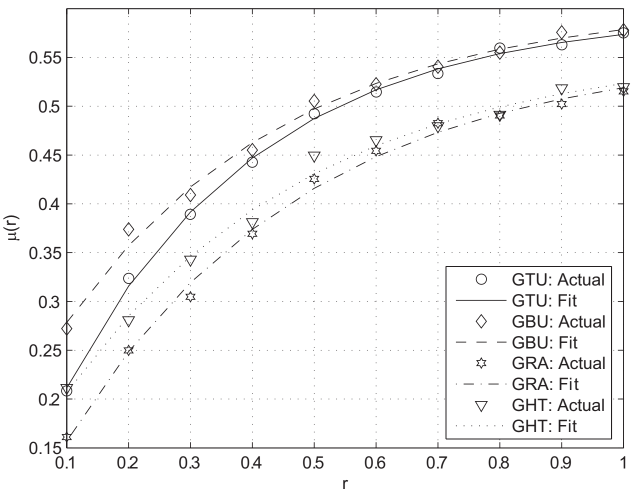

Fig. 5. Mean, $\mu(r)$, of the distance-dependent model of the orthogonality factor, as a function of distance from base station for GTU, GBU, GRA, and GHT environments.

Figure 5 plots the observed $\mu(r)$ for the four environments. It also plots the minimum-mean-square-error parametric curve-fit of the form:

$$\mu(r) = a_1 - a_2 \exp(-r/\gamma). \quad (11)$$

Table II lists the values for a_1, a_2, and γ for the four environments, derived using a minimum mean square error criterion. From the rms errors due to curve-fitting, listed in the last column of the table, it can be seen that the curve-fits are highly accurate. As expected, for a given r, $\mu(r)$ is greater for GBU than GTU, and is greater for GHT than GRA. The functional form also satisfies the intuitive requirement that it should be monotonically increasing and should saturate for large r. Note that these results have a functional form different from the one proposed in [21], in which the median value of the time-averaged OF varied as $\frac{kr}{1+kr}$, where $k = 0.0029/\text{m}$ for $\epsilon = 0.5$.

TABLE II
PARAMETRIC MODEL FOR $\mu(r)$

Environment	a_1	a_2	γ [m]	rms error in $\mu(r)$
GTU	0.596	0.528	316.2	0.0044
GRA	0.558	0.520	3852.1	0.0071
GHT	0.560	0.454	3988.0	0.0084
GBU	0.606	0.432	362.5	0.0074

IV. CONCLUSIONS

We evaluated the statistics of the time-averaged orthogonality factor, $\overline{\beta}_o$, seen at different locations in a cellular area. The ensemble of channel profiles obtained from the general and comprehensive COST259 channel model for macrocells was used for this purpose. The value of $\overline{\beta}_o$ was found to vary over a wide range of values even for a given distance. This suggests that using a single value for the OF in downlink capacity calculations and simulations might lead to misleading conclusions. In general, the OF increased with distance. Upon examining the CDF of $\overline{\beta}_o$ for each environment, we observed that it can be approximately modeled as a truncated Gaussian random variable with a distance-dependent mean and a distance-independent variance. Consequently, $\overline{\beta}_o$ can now be generated directly without having to set up the general, but complex, COST259 macrocellular channel model. While the results in this paper are in the context of cellular system planning for the third generation cellular standard, WCDMA [2], the insights and qualitative conclusions are applicable to other cellular CDMA standards in deployments in which the channels exhibit multiple multipath clusters and have distance-dependent multipath cluster delay spreads. In general, as the bandwidth decreases, the number of resolvable multipaths in the delay profile decreases, which leads to a decrease in the OF.

REFERENCES

[1] X. Qiu, L. F. Chang, Z. Kostic, T. M. Willis, III, L. J. Greenstein, N. B. Mehta, K. Chawla, J. F. Whitehead, and J. Chuang, "Some performance results for the downlink shared channel in WCDMA," in *Proc. ICC*, Apr./May 2002, pp. 376–380.

[2] H. Holma and A. Toskala, *WCDMA for UMTS*. New York: John Wiley, 2000.

[3] K. Sipilä, Z.-C. Honkasalo, J. Laiho-Stefens, and A. Wacker, "Estimation of capacity and required transmission power of WCDMA downlink based on a downlink pole equation," in *Proc. VTC*, May 2000, pp. 1002–1005.

[4] A. F. Molisch, *Wireless Communications*. New York: Wiley-IEEE Press, 2005.

[5] "RF system scenarios," Tech. Rep. 25.942 v6.4.0 (2005-03), 3rd Generation Partnership Project (3GPP).

[6] K. Hiltunen and B. De Ricardo, "WCDMA downlink capacity estimation," in *Proc. VTC*, May 2000, vol. 2, pp. 992–996.

[7] N. B. Mehta, L. J. Greenstein, T. M. Willis, III, and Z. Kostic, "Analysis and results for the orthogonality factor in WCDMA downlinks," *IEEE Trans. Wireless Commun.*, vol. 2, no. 6, pp. 1138–1149, Nov. 2003.

[8] "Deployment aspects," Tech. Rep. 25.943 v6.0.0 (2004-12), 3rd Generation Partnership Project (3GPP).

[9] O. Awoniyi, N. Mehta, and L. Greenstein, "Characterizing the orthogonality factor in WCDMA downlinks," *IEEE Trans. Wireless Commun.*, vol. 2, no. 4, pp. 621–625, July 2003.

[10] S. Kishore, L. J. Greenstein, H. V. Poor, and S. C. Schwartz, "Downlink user capacity in a CDMA macrocell with a hotspot microcell," in *Proc. Globecom*, Dec. 2003, vol. 3, pp. 1573–1577.

[11] L. Greenstein, V. Erceg, Y. Yeh, and M. Clark, "A new path-gain/delay-spread propagation model for digital cellular channels," *IEEE Trans. Veh. Technol.*, vol. 46, no. 2, pp. 477–485, May 1997.

[12] A. Algans, K. I. Pedersen, and P. E. Morgensen, "Experimental analysis of joint statistical properties of azimuth spread, delay spread, and shadow fading," *IEEE J. Select. Areas Commun.*, vol. 20, no. 3, pp. 523–531, Apr. 2002.

[13] U. Martin, "Spatio-temporal radio channel characteristics in urban macrocells," in *IEE Proc. Radar, Sonar and Navigation*, 1999, pp. 42–49.

[14] A. Kuchar, J. P. Rossi, and E. Bonek, "Directional macro-cell channel characterization from urban measurements," *IEEE Trans. Antennas Propagat.*, vol. 48, no. 2, pp. 137–146, Feb. 2000.

[15] K. Kalliola, J. Laurila, M. Toeltsch, K. Hugl, P. Vainikainen, and E. Bonek, "3-D directional wideband dual-polarized measurement of urban mobile radio channel with synthetic aperture technique," in *Proc. Millennium Conference on Antennas & Propagation*, Apr. 2000.

[16] M. Steinbauer and A. F. Molisch, "Directional Channel Modelling." Ch. 3.2 in *Wireless Flexible Personalised Communications. COST259: European Co-operation in Mobile Radio Research*, L. M. Correia, ed. New York: John Wiley, 2001.

[17] A. F. Molisch, H. Asplund, R. Heddergott, M. Steinbauer, and T. Zwick, "The COST259 directional channel model - I. Overview and methodology," *IEEE Trans. Wireless Commun.*, to appear.

[18] H. Asplund, A. A. Glazunov, A. F. Molisch, K. I. Pedersen, and M. Steinbauer, "The COST259 directional channel model - II. Macrocells," *IEEE Trans. Wireless Commun.*, to appear.

[19] A. A. Glazunov, H. Asplund, and J.-E. Berg, "Statistical analysis of measured short-term impulse response functions of 1.88 GHz radio channels in Stockholm with corresponding channel model," in *Proc. VTC*, Sep. 1999, vol. 1, pp. 107–111.

[20] "Spatial channel model for multiple input multiple output (MIMO) simulations," Tech. Rep. 25.996, 3rd Generation Partnership Project (3GPP).

[21] K. I. Pedersen and P. E. Mogensen, "The downlink orthogonality factors influence on WCDMA system performance," in *Proc. VTC (Fall)*, Sep. 2002, pp. 2061–2065.

[22] C. Passerini and G. Falciasecca, "Modeling of orthogonality factor using ray-tracing predictions," *IEEE Trans. Wireless Commun.*, vol. 3, pp. 2051–2059, Nov. 2004.

[23] C. Passerini and G. Falciasecca, "Correlation between delay-spread and orthogonality factor in urban environments," *IEEE Electron. Lett.*, vol. 37, pp. 384–386, Mar. 2001.

[24] M. Humukumbure, M. Beach, and B. Allen, "Downlink orthogonality factor in UTRA FDD systems," *IEEE Electron. Lett.*, vol. 38, pp. 196–197, Feb. 2002.

[25] H. M. El-Sallabi, J. Sallo, and P. Vainikainen, "Investigations on impact of bandwidth on orthogonality factor for WCDMA systems," in *Proc. WCNC*, Mar. 2004, pp. 1138–1142.